

Synthesis of Dual Stimuli-Responsive Amphiphilic Particles through Controlled Semi-Batch Emulsion Polymerization

Chun Ho Yam, Cheng Hao Lee, Yuen Shan Siu, Kin Man Ho, Pei Li*

Department of Applied Biology and Chemical Technology, The Hong Kong Polytechnic University, Hung Hom, Kowloon, Hong Kong, P. R. China

Corresponding author: Pei Li, E-mail: pei.li@polyu.edu.hk

Abstract

The synthesis and property of dual stimuli-responsive amphiphilic particle consisting of a hydrophobic component, a pH-sensitive poly(ethyleneimine) (PEI) and a temperature-sensitive poly(*N*-isopropyl acrylamide) (PNIPAm) have been investigated. This novel type of multicomponent polymer (MCP) particles were prepared through a one-pot controlled semi-batch emulsion polymerization which involved an initial formation of PNIPAm/PEI core-shell nanogel particle via graft copolymerization of *N*-isopropyl acrylamide from PEI, followed by the seeded emulsion polymerization of methyl methacrylate or styrene. Properties of these MCP particles including particle composition, size, size distribution, surface charge, and morphology were systematically examined. The structure of hydrophobic monomer was found to strongly influence the morphology of resultant MCP particles. The multilayered polystyrene/PNIPAm/PEI particles exhibited the unique property of temperature-tunable surface charge. This property was demonstrated through studies of intracellular

uptake of FITC-label PS/PNIPAm/PEI nanoparticles into HeLa cells at 27 and 37 °C. The results provide some insights into the design of future stimulus-responsive nanoparticle-based therapeutics.

Keywords: Temperature-responsive; amphiphilic; multicomponent; cellular uptake; Polyethyleneimine

1. Introduction

Nano- and micrometer-scale multicomponent polymer (MCP) particles have received increasing attention because of their multiple functionalities, intriguing hierarchical nanostructures, and the synergistic properties of their different components [1]. As there are only a few polymer-polymer pairs that are compatible, various synthetic approaches have been developed to construct MCP particles with different morphologies such as spherical, ellipsoidal, disc-, raspberry-, mushroom-, snowman-, dumbbell-shaped anisotropic, and Janus particles. [2-3]. Furthermore, nanostructures of the MCP particles including core-shell, multi-layered and interpenetrating networks have been tailor-made [4-7]. Among the various types of MCP particles, dual stimuli-responsive MCP particles are of particular interest because of their potential applications in the biological field [8-12]. Thus, advances in the design and engineering of stimuli-responsive nanoparticles as multicomponent constructs, as well as in the understanding of the importance of nanoparticle characteristics such as size, morphology, and surface properties for biological interactions will create new opportunities for the development of nanoparticles for therapeutic applications.

Synthetic methods to prepare dual stimuli-responsive MCP particles containing water-soluble pH- and temperature-sensitive polymers mainly utilize the “graft-from” and “graft-to” strategies [7]. With the rapid development of the surface-initiated polymerization technique, the surface-initiated controlled/living radical polymerization can produce polymer brushes with a high level of control and versatility [13-14]. However, current approaches for generating smart MCP particles are usually quite complicated and involve tedious procedures, thus they are not amendable for production scale-up. Therefore, it is in our interests to develop a ready-to-scale-up method that can efficiently produce amphiphilic particles with pH- and temperature-responsive properties through a one-pot controlled semi-batch emulsion polymerization. This work is built on our previously established method for the synthesis of pH- and temperature-sensitive core-shell nanogels [15]. Effects of crosslinking density of seed nanogel, the structure of hydrophobic monomer, and particle composition on particle size, size distribution, surface charge, and morphology were systematically characterized. The property of temperature-tunable surface charge of the multilayered PS/PNIPAm/PEI particles was also evaluated for their thermally-triggered cellular uptake into HeLa cells.

2. Material and methods

2.1. Materials

Phenolic inhibitors in both methyl methacrylate (MMA) and styrene (St) (Sigma Aldrich) were removed by washing the monomers first with 10 w/w% sodium hydroxide (NaOH) three times, then with deionized water until the pH of the water layer dropped to 7. *N*-isopropylacrylamide (NIPAm, 97%, Wako Pure Chemical Industries) was

purified by a recrystallization method as follows: NIPAm monomer was repeatedly dissolved and crystallized (three times) in a mixture of toluene and hexane (1:5 v/v) to give a spindle-like crystal. Polyethylenimine (PEI, weight average molecular weight of 750,000 g/mol, 50 w/w% solution in water, Sigma Aldrich), *tert*-butyl hydroperoxide (TBHP, 70 w/w% solution in water, Sigma Aldrich), fluorescein isothiocyanate isomer (FITC, Sigma Aldrich), and *N,N'*-methylenebis(acrylamide) (MBA, 98%, BDH) were all used as received. Freshly deionized Milli-Q water was used as the dispersion medium. Dulbecco's modified Eagle's medium (DMEM, high glucose), fetal bovine serum (FBS, E.U.-approved, South America origin) and Penicillin/Streptomycin (P/S, 10,000 U/mL), were purchased from ThermoFisher Scientific. Human cervix adenocarcinoma (HeLa) cells were obtained from the American Type Culture Collection.

2.2. Synthesis of PS/ PNIPAm/PEI and PMMA/PNIPAm/PEI multicomponent particles

Particle synthesis was based on a controlled semi-batch seeded emulsion polymerization. A typical procedure is as follows: For a total solution volume of 100 mL, PEI (2 g, 50 w/w% solution) was first dissolved in deionized water, followed by adjustment of the solution pH to 7 with a 2 M HCl solution. The PEI solution was then transferred to a three-necked water-jacketed reaction flask equipped with a thermal couple (Testo 735), a condenser, a magnetic stirrer, and a nitrogen inlet. An appropriate amount of NIPAm with or without MBA crosslinking agent (see recipe in Table S1, Supporting Information) was then charged to the reaction flask. The mixture was stirred at 350 rpm and heated to 80 °C under nitrogen for 30 min. TBHP solution (1 mL, 0.1 M) was added to the mixture to start the polymerization as indicated by the rising

solution temperature (Figures S1 and S2 in Supporting Information). When the first stage of exothermic polymerization had almost completed, the second monomer, styrene or MMA (2 g), was added to the reactor to carry out seeded emulsion polymerization at 80 °C for 2 hours, giving stable MCP latex particles. Monomer conversions of the MCP particles were determined gravimetrically according to the following procedures: latex dispersion (2 mL) was withdrawn from the reaction mixture and dried overnight at 80 °C. It was further dried in a vacuum oven at 50 °C for 3 days. Assuming that all the remaining monomer and other small molecules were removed during the vacuum drying process, the dried solid should contain only MCP particles and unreacted PEI. The total solid content (Total S.C.%) of the latex dispersion was determined, and the monomer conversion was calculated based on the following equation:

$$\text{Monomer Conversion (\%)} = \left(\frac{\text{Total S.C.\%} - \text{S.C.\%}_{\text{PEI}} - \text{S.C.\%}_{\text{HCl}}}{\text{S.C.\%}_{\text{Total monomer}}} \right) \times 100\%$$

Where S.C.%_{PEI} is the amount of PEI initially added; S.C.%_{HCl} is the amount of HCl initially used for pH adjustment; and S.C.%_{Total monomer} is the total amount of monomer added throughout the reaction. The final products were purified by repeated centrifugation (19,500 rpm for 1.5 hours), decantation and re-dispersion until the conductivity of the supernatant was close to that of deionized Milli Q water.

2.3. Synthesis of crosslinked PNIPAm/PEI core-shell nanogels

The crosslinked PNIPAm/PEI nanogel particles used as the seeded particles were synthesized according to the procedure described above except that the first stage of polymerization was carried out in the presence of a crosslinker, *N,N'*-

methylenebis(acrylamide) (MBA). The weight ratios between NIPAm and MBA were varied between 90:10 (10% crosslinking), 95:5 (5% crosslinking) and 98:2 (2% crosslinking).

2.4. Measurement and characterization

2.4.1. Fourier Transformed Infrared (FT-IR) Spectral Studies

The FTIR spectrum was recorded in the transmission mode on a Nicolet 380 FT-IR spectrophotometer. The freeze-dried sample (5 mg) was ground with an appropriate amount of anhydrous KBr and compressed into a pellet under a force of 9 tones for 1 min.

2.4.2. Particle Size Measurement

Particle size and size distribution were determined by a Beckman Coulter DelsaTMNano C Particle Analyzer complemented with a DelsaTMNano Autotitrator. The photon correlation spectroscopy was obtained based on electrophoretic dynamic light scattering from a two-laser diode light source at a wavelength of 632.8 nm and a scattering angle of 165°. Sample concentrations were between 200 and 300 mg/L. Hydrodynamic diameter, D_h , was calculated based on the Einstein Stokes equation $D_h = k_B T / 3\pi\eta D$, where k_B is the Boltzmann constant, T is the temperature (K), η is the viscosity of the dispersing medium, and D is the diffusion coefficient obtained from the decay rate of the intensity correlation function of the scattered light (i.e., correlogram), $G(\tau) = \int I(t)I(t+\tau)dt$. Results of particle size (Z_{AVE}) were an average of triplicate measurements.

2.4.3. zeta-Potential Measurements

Zeta-potential was measured with a Delsa Nano C Particle Analyzer (Beckman Coulter) equipped with a thermal equilibrating device. The correlations between solution temperature and hydrodynamic diameter as well as ζ -potential of the MCP particles were investigated at different temperatures (25 °C, 27 °C, 29 °C, 32 °C, 35 °C, 37 °C, and 39 °C). Each sample was equilibrated at a preset temperature for 10 mins before the measurement.

2.4.4. Scanning Electron Microscopy

The particle morphology, size, and size distribution of the MCP particles in the dry state were examined by a field-emission scanning electron microscope (FE-SEM, JEOL-JSM 6335F). The operating accelerating voltage of FE-SEM was maintained at 5 kV throughout the measurement. Samples were prepared by spreading a small drop of dilute MCP particle dispersion (100 mg/L) on a mica substrate and drying overnight in a dust-free environment at room temperature. The dried samples were then sputtered with a thin layer of gold under vacuum to a depth of approximately 5 Å.

2.4.5. Transmission Electron Microscopy

TEM images of samples were obtained using a transmission electron microscope (JEOL, 100 CXII TEM) at an accelerating voltage of 100 kV. Samples were prepared by wetting carbon-coated grids with a small drop of dilute particle dispersion (10 μ L, 50 mg/L). Upon drying, the samples were stained with 0.5 w/w% phosphotungstic acid

(PTA, $\text{WO}_2 \cdot \text{H}_3\text{PO}_4 \cdot x\text{H}_2\text{O}$) solution for 1 minute, then dried at room temperature before analysis. All TEM images were taken in a bright field mode.

2.5. Cell culture

HeLa cells were cultured in a high glucose Dulbecco's modified Eagle's medium (DMEM) supplemented with 10 v/v% heat-inactivated fetal bovine serum (FBS), 1% penicillin/streptomycin (P/S) at 37 °C in a humidified atmosphere containing 5% CO_2 .

2.6. In vitro cellular uptake studies of the MCP particles

The cellular uptake behavior of the PS/(PNIPAm-2%MBA)/PEI and PMMA/PEI (as positive control) particles was studied with a Leica DMRM fluorescence microscope. The MCP particles were first labeled with a fluorescein isothiocyanate isomer 1 (FITC) at PEI to FITC weight ratio of 2 to 1 through incubation in a borate buffer (0.1 M, pH 8.5) for 4 hours at 27 °C. The unreacted FITC molecules were removed by dialysis against autoclaved Milli-Q water using a dialysis tube with a molecular cut-off of 12,000 Da. HeLa cells were seeded on the 12 mm sterile circular coverslip with an initial density of 1×10^5 cells and incubated overnight. The cells were then treated with FITC-labeled particles at a final concentration of 100 $\mu\text{g/mL}$. Cells without particle treatment or those treated with non-FITC labeled particles would serve as negative controls. Two sets of samples were prepared in a serum-free medium and incubated with cells at 27 °C and 37 °C for 3 hours respectively. Subsequently, the medium was replaced with a complete growth medium, and incubated at 37 °C for another 3 hours. After this post-transfection, cells were washed with 1 x PBS solution,

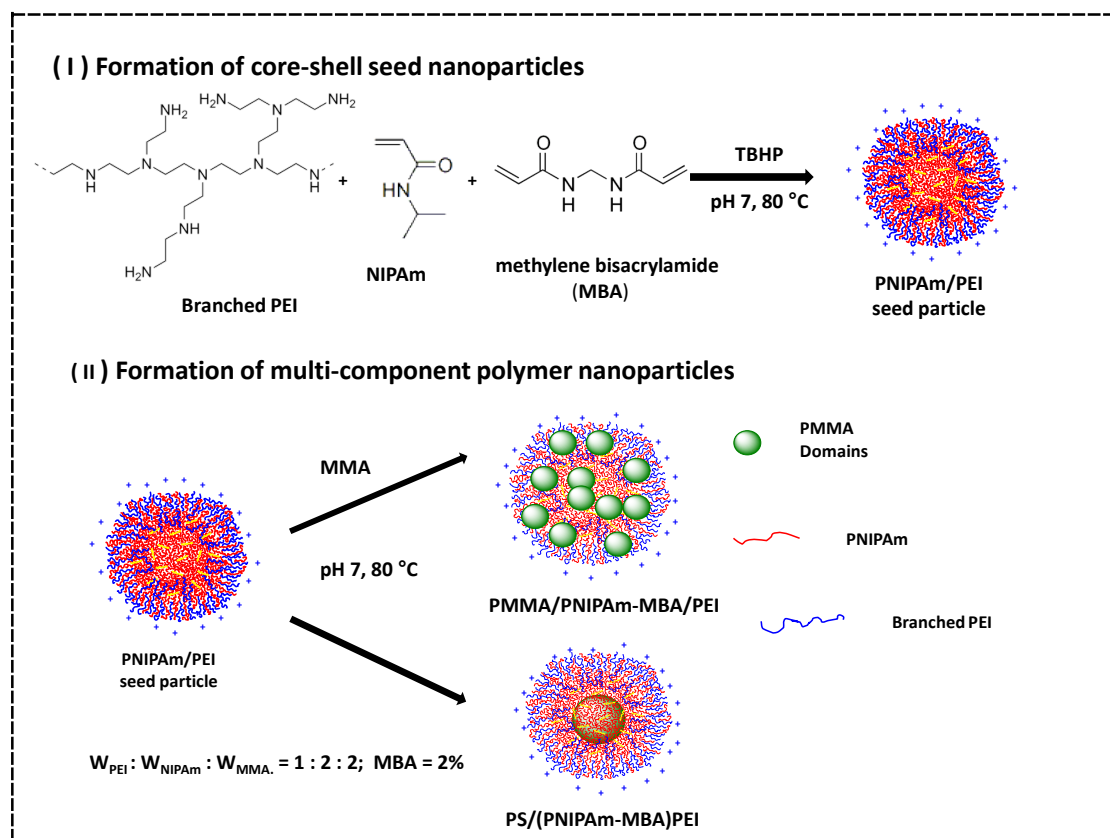
mounted on a microscopic slide, and visualized by the Leica DMRM fluorescence microscope.

3. Results and Discussion

3.1. *Synthesis of MCP particles*

Scheme 1 illustrates the synthetic route to dual stimuli-responsive amphiphilic particles through a one-pot controlled semi-batch emulsion polymerization. In the first stage, seed nanogel particles are formed via graft copolymerization of *N*-isopropyl acrylamide (NIPAm) from PEI in the presence or absence of an MBA crosslinker to generate PNIPAm/PEI nanogels in water. This polymerization mechanism has been comprehensively described in our previous work [15-16]. Since polymerization takes place at 80 °C, a temperature that is higher than the lower critical solution temperature (LCST) of PNIPAm, the PNIPAm chain would shrink and become hydrophobic, thus leading to *in situ* self-assembly of the amphiphilic PEI-*g*-PNIPAm to form micelle-like particles. If the crosslinking monomer, MBA, is present, crosslinked (PNIPAm-MBA)/PEI nanogels can be formed. When the second hydrophobic monomer such as methyl methacrylate and styrene is introduced to the reaction system, the preformed nanogels could act as seed nanoparticles where the hydrophobic monomer can rapidly diffuse from the aqueous phase into the seed nanogel because the monomer has greater compatibility with the seed particle than the water. The swollen seed particles then undergo seeded emulsion polymerization without the need to charge the second batch initiator. This one-pot polymerization can be easily controlled by monitoring changes in reaction temperature during the reaction.

Figures S1 and S2 in Supporting Information illustrate the polymerization schemes and temperature profiles for the synthesis of PMMA/PNIPAm/PEI and PS/PNIPAm/PEI MCP particles in the absence of a crosslinker, respectively. When adding the initiator solution, the reaction temperature immediately dropped to 79.5 °C, followed by increasing to 80.5 °C within 10 mins due to exothermic polymerization of the NIPAm monomer. After about 15 mins, the reaction temperature fell back to the starting temperature, indicating that most of the NIPAm monomer had been polymerized. Subsequently, the second batch of MMA monomer was charged to the reactor which contained the seed nanogels, and started the seeded emulsion polymerization. Similarly, a rapid increase in reaction temperature was recorded, indicating exothermic polymerization of the monomer. It is worth mentioning that even though no extra initiator was charged to the reactor in the second stage, the polymerization was still able to proceed efficiently to high monomer conversion (usually higher than 90%). This phenomenon might be attributed to the low radical termination due to the compartmentalization effect inside the particles [16]. This controlled semi-batch emulsion polymerization is simple, efficient, and amendable to scale-up production.



Scheme 1. Schematic presentation of the syntheses of PS/PNIPAm/PEI and PMMA/PNIPAm/PEI MCP particles via a one-pot controlled semi-batch seed emulsion polymerization.

3.2. Chemical compositions of the MCP particles

The chemical structures of purified (PNIPAm-2%MBA)/PEI seed nanogels, PMMA/PNIPAm/PEI and PS/PNIPAm/PEI particles were identified using an FT-IR spectrometer. The spectrum of seed nanogels (Figure 1a) shows characteristic peaks of PNIPAm (Strong amide carboxyl, 1650 cm^{-1} ; strong N-H amide bending peak, 1545 cm^{-1} ; and isopropyl C-H peak, $1390\text{ to }1370\text{ cm}^{-1}$) and PEI (amine N-H stretching, $3400\text{ to }3500\text{ cm}^{-1}$; and C-H stretching and bending, $2900\text{ to }3000\text{ cm}^{-1}$). The spectrum of the PS/PNIPAm/PEI particles (Figure 1b) exhibits not only characteristic peaks of PNIPAm and PEI, but also additional absorption peaks at $750\text{ and }700\text{ cm}^{-1}$ (aromatic =C-H out-

of-plane bending vibration peaks) and between 2950 and 3050 cm^{-1} ($=\text{C-H}$ vinylic hydrogen), suggesting the presence of polystyrene. Furthermore, the spectrum of the PMMA/PNIPAm/PEI particles (Figure 1c) exhibits not only characteristic peaks of PNIPAm and PEI, but also additional absorption peaks at 1735 cm^{-1} (C=O carbonyl) and between 1150 and 1300 cm^{-1} ($-\text{C-O}-$ ester), indicating the presence of PMMA. Therefore, the chemical compositions of these three types of particles have been confirmed.

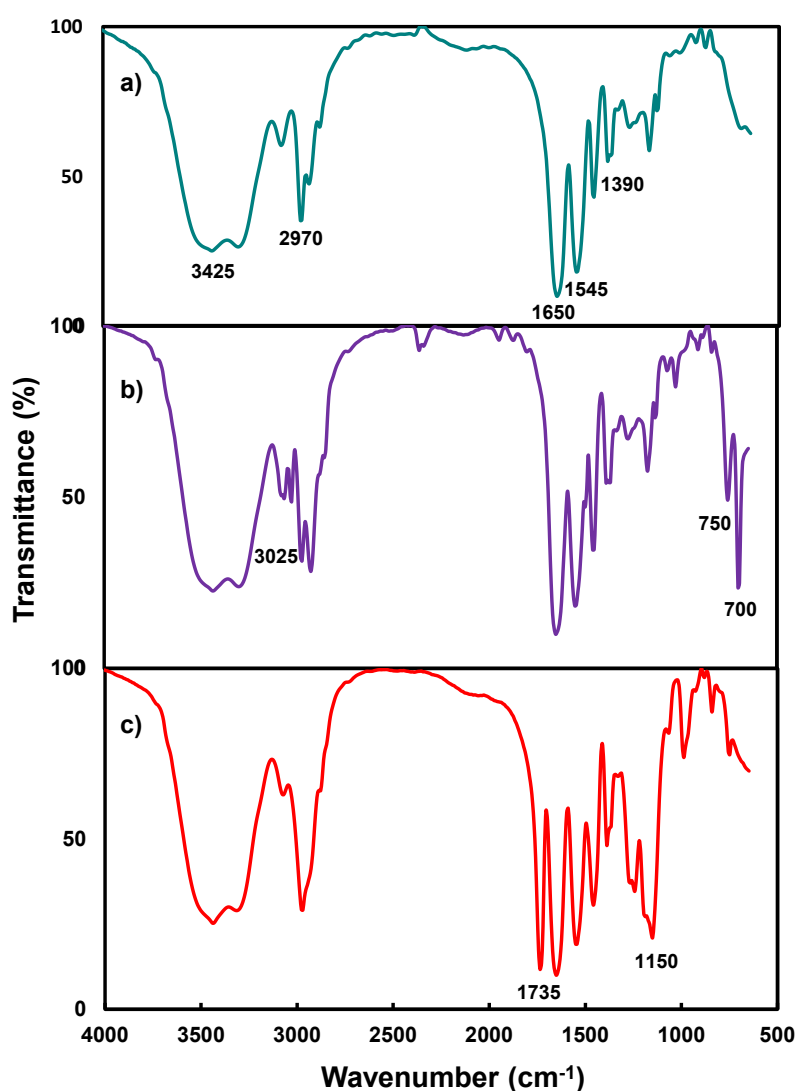


Fig. 1. FT-IR spectra of a) (PNIPAm-2%MBA)/PEI seed nanogels; b) PS/(PNIPAm-2%MBA)/PEI particles; and c) PMMA/(PNIPAm-2%MBA)/PEI particles.

3.3. Particle size and size distribution of seed nanogels and MCP particles

The hydrodynamic diameters (Z_{AVE}) and particle size distribution (PDI) of seed and MCP particles were determined by dynamic light scattering (DLS) at pH 7. Comparing the particle sizes and size distributions of (PNIPAm-2%MBA)/PEI seed nanogels (383.6 nm, PDI = 0.127), PS/(PNIPAm-2%MBA)/PEI (316.6 nm, PDI = 0.041) and PMMA/(PNIPAm-2%MBA)/PEI (352.6 nm, PDI = 0.118) MCP particles (Figure S3 in Supporting Information), it was found that the seed nanogels had bigger average size than the resultant MCP particles with smaller PDI value. These results suggest that the seed particles were highly uniform and very stable in the aqueous system. After polymerizing with the second monomer (styrene or MMA), the resultant MCP particles became smaller than the seed nanogels. Since particle sizes were all measured at room temperature which is below the LCST of PNIPAm, the PNIPAm/PEI seed nanogels were highly swelling under this temperature due to their hydrophilic nature. After introducing the hydrophobic monomer, the presence of hydrophobic polymer in the MCP particle would reduce the nanogel swelling because of the covalent linkage between the hydrophilic and hydrophobic polymers. Results also indicate that PS/(NIPAm-2%MBA)/PEI MCP particles have smaller particle sizes and narrower size distribution than the PMMA/(NIPAm-2%MBA)/PEI MCP particles under the same composition.

3.4. Effect of seed particle crosslinking and second monomer structure on the formation of MCP particles

As mentioned above, seed nanogel particles of PNIPAm/PEI are first generated through the TBHP-initiated graft copolymerization of NIPAm from PEI. In the

presence of a crosslinker, the crosslinked nanogel particles act as seed nanoparticles for subsequent polymerization. Figures 2a and 2b show morphologies of the nanogels with 2% and 5% crosslinking relative to the NIPAm monomer. TEM images exhibit that they are highly uniform particles with a well-defined core-shell nanostructure. The darker core is the PNIPAm while the lighter shell is the PEI. An increase in crosslinking degree from 2% to 5% results in particles with a less well-defined core-shell nanostructure.

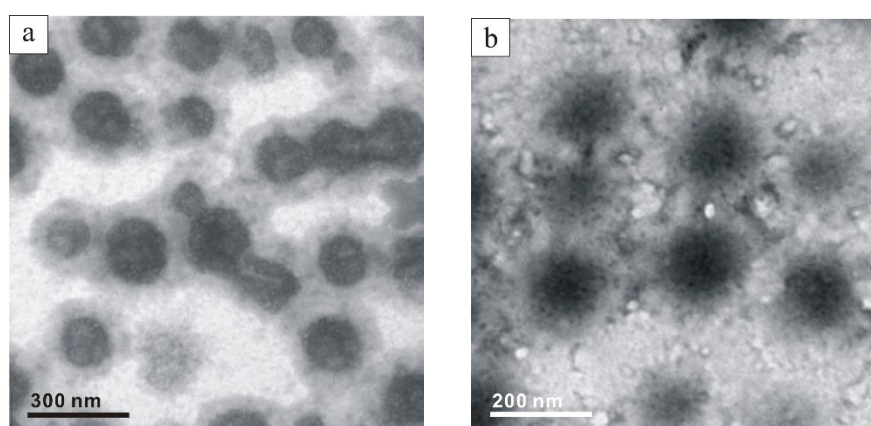


Fig. 2. TEM images of crosslinked PNIPAm/PEI seed nanogels with different MBA crosslinking degrees (relative to the NIPAm monomer): (a) 2% crosslinking; (b) 5% crosslinking. The particles were stained with 0.5 w/w% of the phosphotungstic acid solution for 5 mins.

Upon polymerization of the second monomer, the final morphology of the MCP particles was strongly dependent on the monomer reactivity as well as compatibility between the newly formed polymer and the seed polymer. Since both MMA and styrene are hydrophobic monomers, the newly formed PMMA and PS are incompatible with the existing hydrophilic PNIPAm/PEI nanogels. Thus phase separation of the incompatible polymers could take place during the polymerization, resulting in the

formation of clusters of the newly formed polymer. Figures 3(a-b) show SEM images of the PMMA/PNIPAm/PEI particles with PNIPAm crosslinking degrees of 2% and 5%. The particles appear to have an irregular shape. TEM images in Figure 3(c-e) reveal that each particle contains several nano-domains which are embedded in the corona. The domain (white dot) is the PMMA while the dark corona is composed of interpenetrated PNIPAm and PEI chains. Crosslinking degree of the seed nanogel was found to strongly influence the distribution of the PMMA nano-domains within the particle. Nanogel particles with 5% crosslinking resulted in a higher number of PMMA domains localized on the outer layer (Figure 3c). Lowering the crosslinking degree to 2% or even without crosslinking gave a more even distribution of the PMMA domains in the entire particles (Figures 3d and e). These results suggest that seed nanogels with a higher degree of crosslinking inhibit diffusion of the second stage monomer into the particles and migration of newly formed polymer chains.

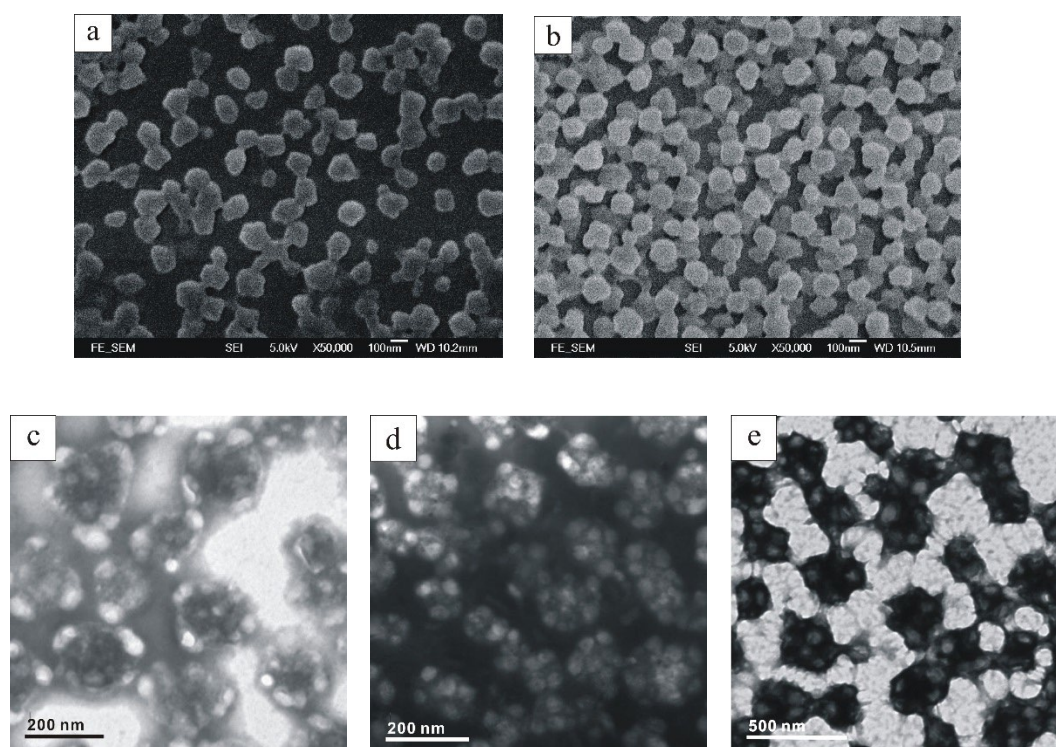


Fig. 3. SEM and TEM images of the MCP particles: a) PMMA/(PNIPAm-5%MBA)/PEI; b) PMMA/(PNIPAm-2%MBA)/PEI; c) PMMA/(PNIPAm-5%MBA)/PEI; d) PMMA/(PNIPAm-2%MBA)/PEI; e) PMMA/PNIPAm/PEI without crosslinking. Particles for TEM observation were stained with 0.5 w/w% PTA solution for 5 mins.

Unlike the PMMA/PNIPAm/PEI MCP particles, the PS/PNIPAm/PEI particles have a spherical shape as shown in Figures 4a and 4b. TEM images further reveal that the particle has multilayer morphology: the inner core (spherical light region) is the polystyrene; the middle layer (dark region) is mainly the PNIPAm; and the outermost layer (hairy region) is the PEI (Figure 4e). Some smaller particles were also found, suggesting that polymerization of styrene might also occur outside of the seed nanogels. Figures 4(c-e) show morphologies of PS/PNIPAm/PEI particles prepared with different crosslinking degrees of the seed nanogels. It was found that the multilayer nanostructure became more and more well-defined with a minimum crosslinking degree.

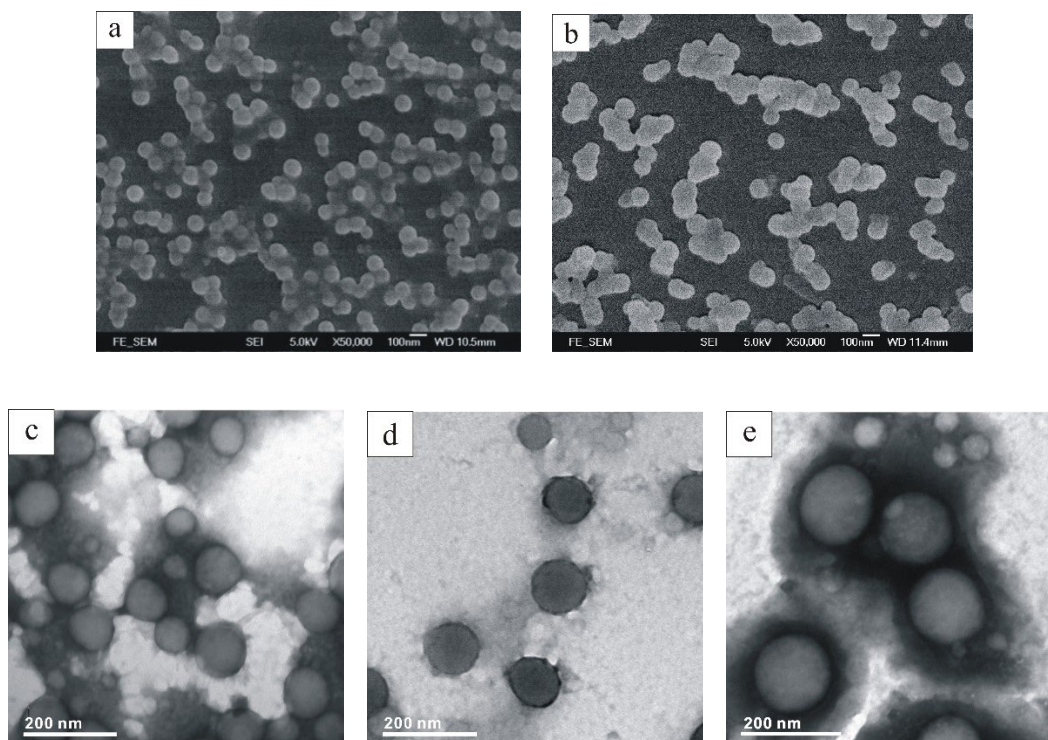


Fig. 4. SEM and TEM images of the PS/PNIPAm/PEI MCP particles: a) PS/(PNIPAm-5%MBA)/PEI; b) PS/(PNIPAm-2%MBA)/PEI; (c) PS/(PNIPAm-5%MBA)/PEI; (d) PS/(PNIPAm-2%MBA)/PEI; (e) PS/PNIPAm/PEI without crosslinking. Particles for TEM observation were stained with 0.5 w/w% PTA solution for 5 mins.

Morphological differences between the PS/PNIPAm/PEI and PMMA/PNIPAm/PEI particles may be explained by the concept of thermodynamic and kinetic morphologies [17-18]. Thermodynamic morphology is also referred to as equilibrium morphology. Particles with this morphology possess the lowest Gibbs free energy and are in the most stable state. Upon seeded emulsion polymerization, some clusters of newly formed incompatible polymer would migrate and coalesce due to the van der Waals' forces and Ostward ripening [19]. If the viscosity of the seed particle is low enough for cluster migration, thermodynamic morphology could be developed. Kinetic morphology means non-equilibrium morphology which does not possess minimum interfacial energy.

Although the particles with kinetic morphology are at the meta-stable state, they are still stable enough to maintain the particle morphology. One of the factors that determine the morphology evolution of the particle is the propagation rate of the second-stage monomer. In the case of styrene, since it has a slow propagation rate, seed particles can be effectively swelled. As a result, the viscosity of the polymer matrix is reduced, favoring cluster migration and coalescence. The lower crosslinking density of the seed particle, the lower the viscosity of the polymer matrix would become, and the easier the cluster migration and coalescence would take place. Therefore, PS/PNIPAm/PEI particles without crosslinking could eventually reach the thermodynamic morphology with well-defined multilayer particle morphology. In the case of using MMA as the hydrophobic monomer, since the MMA monomer has a fast propagation rate at 80 °C, the rate of polymerization may be much faster than the rate of diffusion. The fast polymerization of MMA results in the formation of rigid PMMA domains within the PNIPAm/PEI nanogel particles. Thus the PMMA chains are hard to diffuse and coagulate, resulting in the formation of a kinetic morphology.

3.5. Shielding Effect of particle surface charges

As mentioned above, the PS/PNIPAm/PEI MCP particles possess multilayered morphology: the inner core is mainly the polystyrene; the middle layer is the PNIPAm, and the outermost layer is the PEI. Since crosslinking degree of the PNIPAm was very low (e.g., 2% crosslinker relative to NIPAm), the PNIPAm mainly existed either as a graft polymer (PEI-g-PNIPAm) or as a homopolymer in the interior of the particle. The grafted PNIPAm chains and hydrophilic PEI are expected to form the hydrophilic shell. Thus the highly mobile and hydrated PNIPAm chains may be able to shield the surface charges of the PEI at room temperature. Below the LCST of PNIPAm, the graft

PNIPAm chains could swell and interpenetrate with PEI in the particle shell, thus shielding the charge of PEI. When increasing the solution temperature above 32 °C, the PNIPAm graft chains shrink, resulting in the exposure of the PEI chains on the particle shell. To verify this effect, ζ -potential values of PS/PNIPAm/PEI particles comprising three different compositions were determined at different solution pHs (Figure 5). For particles synthesized with 20 w/w% NIPAm (PEI : NIPAm : styrene weight ratio of 1 : 1 : 3), their ζ -potential values are very sensitive to solution pH. An almost linear decrease in ζ -potential value was found when increasing the solution pH from 4.5 to 10. These results suggest that the outmost layer of this type of MCP particle contains predominantly the PEI chains. In other words, the amount of PNIPAm in this composition was still insufficient to shield the protonated amino groups of PEI on the particle surface. When increasing the NIPAm composition to 40 w/w% (PEI : NIPAm : styrene weight ratio of 1 : 2 : 2), a considerable drop in the magnitude of ζ -potential was found. The surface charges became less sensitive to pH changes. Further increasing the NIPAm composition to 60 w/w% (PEI : NIPAm : styrene weight ratio of 1 : 3 : 1) resulted in the reduction of the particle surface charges to almost neutral (between 0 and +5 mV) in pH ranging from 3 to 10. These results suggest that the shielding effect of the PEI by the PNIPAm chains is achievable with the appropriate particle composition. Moreover, the presence of the hydrophilic PNIPAm at the outermost shell was able to provide sufficient particle stability. The above results suggest that the surface charges of the PS/PNIPAm/PEI MCP particles could be tuned by varying the NIPAm composition in the MCP particles.

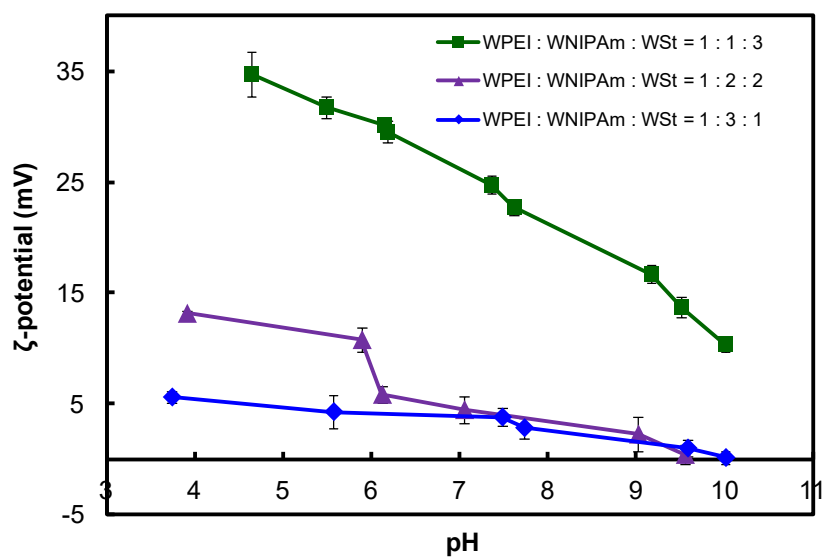
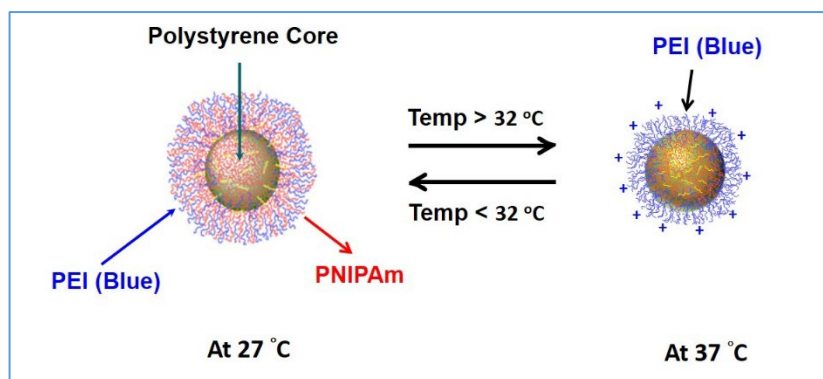


Fig. 5. ζ -potential as a function of pH of PS/PNIPAm/PEI MCP particles

3.6. Temperature Tunable Surface property

A schematic representation of morphological changes of the PS/PNIPAm/PEI MCP particles at 27 and 37 °C is shown in Scheme 2. The PNIPAm chains are highly swollen at 27 °C (below the LCST), resulting in the shielding of the particle surface charges. When the solution temperature is at 37 °C (high than the LCST), the PNIPAm chains would contract toward the hydrophobic polystyrene cores. As a result, the water-soluble PEI chains that co-exist in the particle shell could be fully exposed on the outmost shell, giving highly positive surface charges.



Scheme 2. Schematic presentation of temperature-responsive surface charge property

To illustrate this temperature-responsive surface charge property, non-crosslinked PS/PNIPAm/PEI particles were examined by measuring their surface charges at different temperatures between 25 and 40 °C. Figure 6 shows ζ - potential values of the particles comprising three different compositions as a function of solution temperature. The multilayered PS/PNIPAm/PEI particles with PEI : NIPAm : styrene weight ratios of 1 : 2 : 2 and 1 : 3 : 1 could alter their ζ - potential values from +5 mV and +1 mV to +35 and +27 mV, respectively. This property is attributed to the fact that below the LCST of the PNIPAm, the PNIPAm chains could fully swell in water, resulting in the shielding of the positive charges of the PEI in the outermost shell. When increasing the solution temperature to above 32 °C, the PNIPAm chains could contract toward the inner cores, while the hydrophilic PEI chains remain soluble in water, giving highly positive MCP particles.

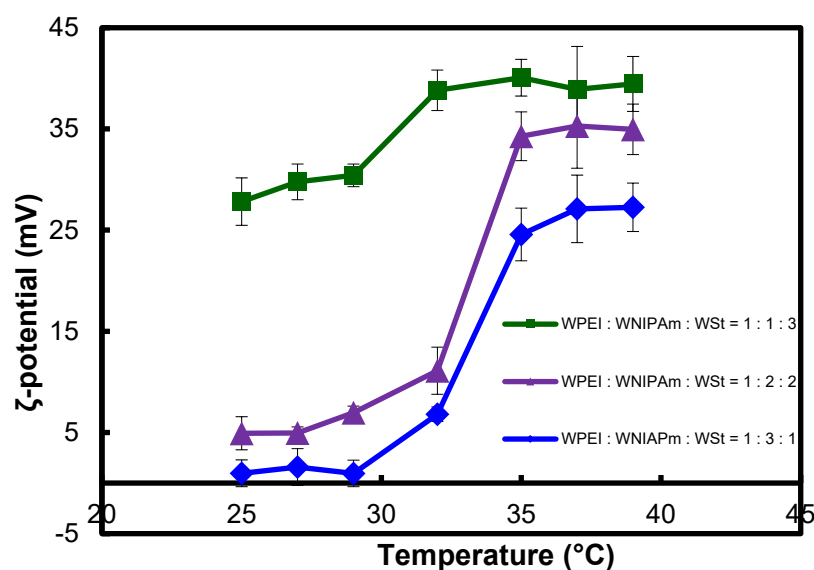


Fig. 6. ζ -Potential values of PS/PNIPAm/PEI MCP particles as a function of solution temperature.

3.7. Thermally-triggered intracellular uptake

Nowadays, advances in the design and engineering of nanoparticles such as multifunctional and three-dimensional constructs, as well as an understanding of the importance of nanoparticle characteristics such as size, shape, and surface properties for biological interactions, are creating new opportunities for the development of nanoparticles for therapeutic applications [20-21]. In the past decade, we have been developing PEI-based amphiphilic core-shell nanoparticles with diameters in the range of 100 to 300 nm as potential nanocarriers for gene and drug deliveries [22-26]. Our results show that these types of nanoparticles are efficient and inexpensive nanocarriers for nucleic acid-based therapies. However, the highly positive surface charge and cytotoxicity of the PEI-based nanoparticles are still major drawbacks in the development of PEI nanoparticle-based therapeutics. To address these problems, we have evaluated the intracellular uptake of PS/PNIPAm/PEI particles at temperatures

below and above the LCST of PNIPAM. The rationale of this study is that the particles possess a strong temperature-responsive surface charge. Below the LCST of the PNIPAm (around 32 °C), particle surface charges are very low due to the shielding effect of the neutral PNIPAm chains. Raising the temperature to above LCST of the PNIPAm leads to contraction of the PNIPAm chains towards the particle core, thus exposing the cationic PEI chains. The resulting positive surface charges could facilitate intracellular uptake. Another advantage of this type of pH- and temperature-dual responsive nanoparticles is that the shielding of the PEI surface charge can sterically prevent non-specific interactions in the biological environment, thus prolonging the half-life of the carriers in the bloodstream [27].

Figure 7 shows temperature dependence on both particle size and surface charge of the PS/(PNIPAm-2%MBA)/PEI particles. The hydrodynamic diameters of the particles are 317 and 272 nm at 25 and 39 °C, respectively. Thus there is a 14% size reduction with these temperature changes. For the surface charge property, the ζ -potential value is +16.5 mV at 25 °C, but greatly increases to +39.8 mV at 39 °C. These results suggest that variation in surface charges is quite significant.

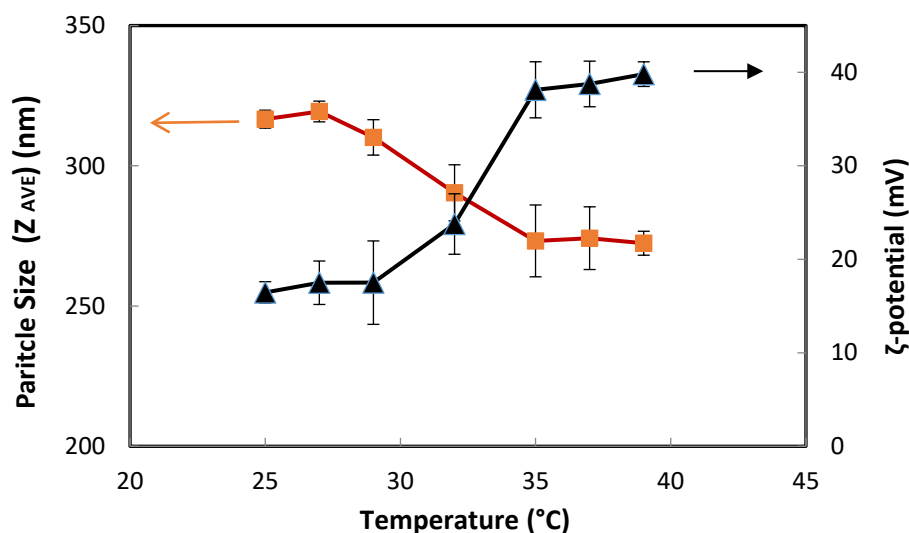


Fig. 7. Effect of temperature on the particle size (■) and surface charge (▲) of the PS/(PNIPAm-2%MBA)/PEI particles.

To apply this unique property for thermally-triggered intracellular uptake, we have labeled the PS/(PNIPAm-2%MBA)/PEI particles with a fluorescence probe, fluorescein isothiocyanate isomer 1 (FITC), through covalent linkages between isothiocyanate groups of the FITC molecules and primary amines of the PEI molecule (Reaction scheme is shown in Figure S4 in Supporting Information). *In vitro* intracellular uptake and distribution of the FITC-labeled MCP particles in HeLa cells were tracked with fluorescence microscopy. Untreated HeLa cells and HeLa cells treated with unlabeled particles served as negative controls. No fluorescence signals were observed at either incubation temperatures of 27 or 37 °C, confirming that neither the HeLa cells nor MCP particles were auto-fluoresce under the experimental conditions (Figure 8). We have also used PMMA/PEI-FITC core-shell particles as a positive control in this study to eliminate the influence of temperature on the cellular uptake process. Figure 8 displays green fluorescence signals for cells transfected at 27

°C, suggesting that the PMMA/PEI-FITC was able to be internalized into cells at this temperature. With increasing the transfection temperature to 37 °C, the green fluorescence signal intensity was enhanced, indicating that the cellular uptake process is slightly more active at 37 °C. When the HeLa cells were treated with FITC-labeled PS/(PNIPAm-2%MBA)/PEI MCP particles at 27 °C, almost no fluorescent signal was observed in the HeLa cells, indicating that the MCP particles were unable to be internalized into the HeLa cells under this temperature. However, when the transfection temperature was raised to 37 °C, an intense green fluorescence signal was observed in both cytoplasmic and nuclear regions of the HeLa cells. Some particles were even translocated from the cytoplasm into the nucleus.

The above results suggest that cationic PEI at the outermost shell of the MCP particle is a critical parameter to trigger intracellular uptake of the particles. At 27 °C, the outermost shells of MCP particles contain both the PNIPAm and PEI chains. Thus the cationic charges of PEI are largely shielded by the PNIPAm chains, giving a nearly neutral particle surface. As a result, the interaction between the particle and cell surface is very weak. When increasing the temperature to 37 °C, shrinkage of the PNIPAm chains leads to exposure of the cationic PEI on the particle surface. The resulting positive surface charges enable effective intercellular uptake of the MCP particles as is evident from the strong fluorescence signal in HeLa cells. This temperature-dependent surface charge property may allow us to exploit targeted and selective delivery through local heating (e.g. by infrared irradiation). Further research on the use of this type of multilayered MCP particles with a phase transition temperature slightly above physiological temperature may lead to an efficient and versatile nanocarrier for targeting and selective drug/gene deliveries [28].

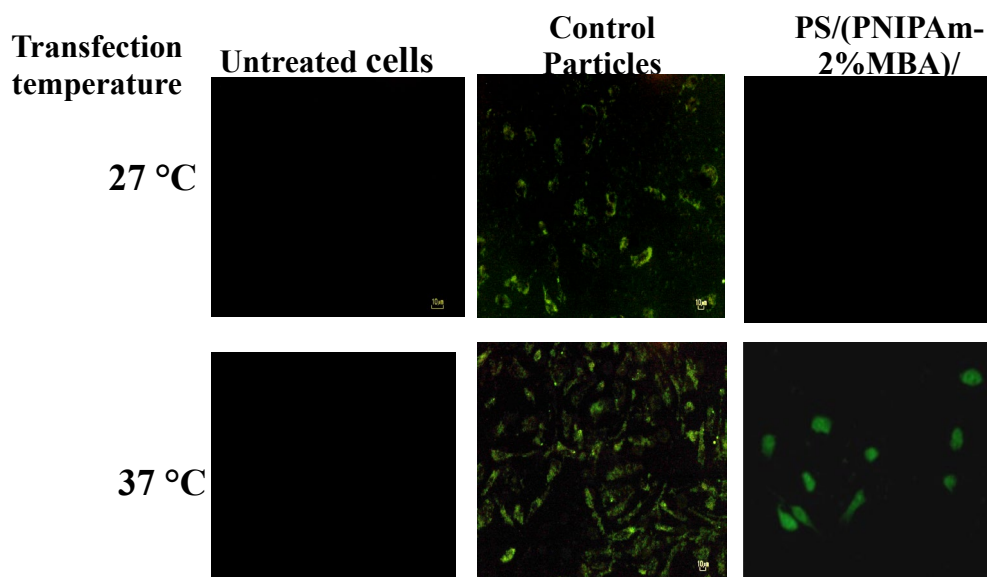


Fig. 8. Fluorescence microscopic images of HeLa cells: Untreated HeLa cells at 27 and 37 °C; Positive control of HeLa cells treated with PMMA/PEI-FTIC; and FITC-labeled PS/(PNIPAm-2%MBA)/PEI particles in HeLa cells (transfection temperatures were at 27 and 37 °C).

4. Conclusion

The synthesis of dual stimuli-responsive amphiphilic particles that consist of a hydrophobic component [polystyrene or poly(methyl methacrylate)], a pH-sensitive poly(ethyleneimine) and a temperature-sensitive poly(*N*-isopropyl acrylamide) has been developed through a one-pot controlled semi-batch emulsion polymerization. The polymerization involved the initial formation of PNIPAm/PEI seed nanogel particles with a well-defined core-shell nanostructure via graft copolymerization of *N*-isopropyl acrylamide from PEI, followed by the addition of either the methyl methacrylate or styrene monomer to undergo a seeded emulsion polymerization. Morphologies of the resultant MCP particles were strongly dependent on the crosslinking degree of the seed nanoparticle and the chemical structure of the hydrophobic monomer. Addition of

MMA in the second stage of seed emulsion polymerization generated PMMA/PNIPAm/PEI particles with multi-domain nanostructure, while the use of styrene gave multilayered polystyrene/PNIPAm/PEI particles. Variation of PNIPAm composition in the multilayered MCP particles could provide charge shielding and temperature tunable surface properties. Thermally triggered intracellular uptake was demonstrated using FITC-labeled PS/(PNIPAm-2%MBA)/PEI particles at 27 and 37 °C. Further investigation on the effect of the temperature-responsive surface of this type of PEI-based nanoparticles on intracellular uptake, cellular distribution, and stability is still ongoing. Results from these studies may provide useful insights into the design of future stimulus-responsive nanoparticle-based therapeutics.

Acknowledgments

This work was supported by the Hong Kong Polytechnic University and PolyU Lo Ka Chung Centre for Natural Anti-Cancer Drug Development.

Appendix A. Supplementary data

Supplementary data related to this article can be found at ...

References

- [1] S. Saha and S. C. J. Loo, Recent developments in multilayered polymeric particles – from fabrication techniques to therapeutic formulations, *J. Mater. Chem. B* 3 (2015) 3406-3419.

- [2] M. J. Monteiro, M. F. Cunningham, Polymer Nanoparticles via Living Radical Polymerization in Aqueous Dispersions: Design and Applications, *Macromolecules* 45(12) (2012) 4939-4957.
- [3] J. Du, R. K. O'Reilly, Anisotropic particles with patchy, multicompartiment and Janus architectures: preparation and application, *Chem. Soc. Rev.* 40(5) (2011) 2402-2416.
- [4] D.I. Lee, Nanostructured latexes made by a sequential multistage emulsion polymerization, *J. Polym.Sci. A Polym. Chem.* 44(9) (2006) 2826-2836.
- [5] R. Hu, V. L. Dimonie, M. S. El-Aasser, R. A. Pearson, A. Hiltner, S. G. Mylonakis, L. H. Sperling, Multicomponent latex IPN materials. I. Morphology control, *J. Polym.Sci. A Polym. Chem.* 35(11) (1997) 2193-2206.
- [6] Y. Chen, N. Ballard, F. Gayet, S.A.F. Bon, High internal phase emulsion gels (HIPE-gels) from polymer dispersions reinforced with quadruple hydrogen bond functionality, *Chem. Commun.* 48(8) (2012) 1117-1119.
- [7] K. M. Ho, W. Y. Li, P. Li, Amphiphilic polymeric particles with core-shell nanostructures: emulsion-based synthesis and potential applications, *Colloid and Polym. Sci.* 288 (2010) 1503-1523.
- [8] X. Wang, D. Niu, C. Hu, P. Li, Polyethyleneimine-based nanocarriers for gene delivery, *Curr. Pharm. Design* 21 (2015) 6140-6156.
- [9] R. Cheng, F. Meng, C. Deng, H. Klok, Z. Zhong, Dual and Mult-stimuli Responsive Polymeric Nanoparticles for Programmed Site-Specific Drug Delivery, *Biomaterials* 34 (2013) 3647-3657.
- [10] S. Ganta, H. Devalapally, A. Shahiwala, M. Amiji, A Review of Stimuli-Responsive Nanocarriers for Drug and Gene Delivery, *J. of Control. Rel.* 126 (2008) 187-204.

- [11] Z. Xing, C.Wang, J. Yan, L. Zhang, L. Li, L. Zha, Dual Stimuli Responsive Hollow Nanogels with IPN Structure of Temperature Controlling Drug Loading and pH Triggering Drug Release, *Soft Matter* 7 (2011) 7992-7997.
- [12] X. Huang, X. Jiang, Q. Yang, Y. Chu, G. Zhang, B.Yang, R. Zhuo, Triple-stimuli (ph/temp/reduction Sensitive Copolymers for Intracellular Drug Delivery *J. Mater. Chem. B.* 1 (2013) 1860-1868.
- [13] Z. Qu, H. Xu, H. Gu, Synthesis and Biomedical Applications of Poly(methacrylic acid) Brushes, *ACS Appl. Mater. Interfaces* 7 (2015) 14537-14551.
- [14] P. B. Zetterlund, S. C. Thickett, S. Perrier, E. Bourgeat-Lami, Controlled/Living Radical Polymerization in Dispersed Systems: An Update, *Chem. Rev.* 115 (2015) 9745-9899.
- [15] M. F. Leung, J. Zhu, F. W. Harris, P. Li, New route to smart core-shell polymeric microgels: Synthesis and properties, *Macromol. Rapid Commun.* 25 (2004) 1819–1823.
- [16] K. M. Ho, W. Y. Li, C. H. Lee, C. H. Yam, R. G. Gibert,, P. Li, Mechanistic study of the formation of amphiphilic core–shell particles by grafting methyl methacrylate from polyethylenimine through emulsion polymerization, *Polymer* 51 (2010) 3512–3519.
- [17] Y. Reyes, J. M. Asua, Modeling Multiphase Latex Particle Equilibrium Morphology, *J. Polym.Sci. A Polym. Chem.* 48 (2010) 2579–2583.
- [18] J. M. Stubbs, D. C. Sundberg, The dynamics of morphology development in multiphase latex particles, *Prog. in Org. Coatings* 61 (2008) 156–165.
- [19] D. C. Sundberg, Y. G. Durant, Latex Particle Morphology, Fundamental Aspects: A Review, *Polym. React. Eng.* 11 (2003) 379–432.

- [20] J. Ramos, J. Forcade, R. Hidalgo-Alvarez, Cationic Polymer Nanoparticles and Nanogels: From Synthesis to Biotechnological Application, *Chem. Rev.* 114 (2014) 367-428.
- [21] N. Desai, Challenges in Development of Nanoparticle-Based Therapeutics, *The AAPS Journal* 14 (2012) 282-295.
- [22] J. Zhu, A. Tang, L. P. Law, M. Feng, K. M. Ho, D. K. L. Lee, F. W. Harris, P. Li, Amphiphilic Core-shell Nanoparticles with Poly(ethylenimine) Shells as Potential Gene Delivery Carriers, *Bioconjug. Chem.* 16 (2005) 139-146.
- [23] M. Feng, P. Li, Amine-containing core-shell nanoparticles as potential drug carriers for intracellular delivery, *J. Biomed. Mater. Res.* 80 (2007) 184-193.
- [24] Y. S. Siu, L. Li, M. F. Leung, K. L. D. Lee, P. Li, Polyethyleneimine-Based Amphiphilic Core-Shell Nanoparticles: Study of Gene Delivery and Intracellular Trafficking, *Biointerphases* 7 (2012) 16.
- [25] H. Mimi, K. M. Ho, Y. S. Siu, A. Wu, P. Li, Polyethyleneimine-Based Core-Shell Nanogels: A Promising siRNA Carrier for Argininosuccinate Synthetase mRNA Knockdown in HeLa Cells”, *J. of Control. Rel.* 158 (2012) 123-130.
- [26] Z. Liu, D. Niu, J. Zhang, W. Zhang, Y. Yao, X. Wang, P. Li, J. Gong, Amphiphilic Core-Shell Nanoparticles Containing Dense Polyethyleneimine Shells for Efficient Delivery of MicroRNA to Kupffer Cells, *Int. J. of Nanomed.* 11 (2016) 2785-2797.
- [27] J. M. Harris, R. B. Chess, Effect of Pegylation on Pharmaceuticals, *Nat. Rev. Drug Discovery* 2 (2003) 214-221.

- [28] V. Torchilin, Multifunctional and Stimuli-Sensitive Pharmaceutical Nanocarriers, *Eur. J. of Pharm. and Biopharm.* 71 (2009) 431-444.